Unraveling antiviral efficacy of multifunctional immunomodulatory triterpenoids against SARS-COV-2 targeting virus-specific enzymes

Shweta Choudhary[1], Sanketkumar Nehul[1], Ankur Singh[1], Prasan Kumar Panda[3], Pravindra Kumar[1*], Gaurav Kumar Sharma[2*], Shailly Tomar[1*]

[1]Department of Biosciences and Bioengineering, Indian Institute of Technology Roorkee, Uttarakhand (247667), India.
[2]Indian Veterinary Research Institute, Izatnagar, Bareilly, Uttar Pradesh (243122), India
[3]All India Institute of Medical Sciences, Rishikesh, Uttarakhand (249203), India

***Corresponding author details**

Pravindra Kumar*
Professor and Head of the Department,
Department of Biosciences and Bioengineering,
Indian Institute of Technology Roorkee,
Uttarakhand, India 247667
Email: pravindra.kumar@bt.iitr.ac.in
Telephone: +91-1332-286286
ORCID ID: 0000-0003-2128-7736

Gaurav Kumar Sharma*
Senior scientist,
Centre for Animal Disease Research and Diagnosis (CADRAD),
Indian Veterinary Research Institute, Bareilly (IVRI, Bareilly),
Uttar Pradesh, India (243122)
Telephone: 0581-2302188
Email: gaurvet@gmail.com
ORCID ID: 0000-0002-9996-9422

Shailly Tomar*
Professor,
Department of Biosciences and Bioengineering,
Indian Institute of Technology Roorkee,
Uttarakhand, India 247667
Tel: +91-1332-285849
Fax: 91-1332-273560
Email: shailly.tomar@bt.iitr.ac.in
ORCID ID: 0000-0002-1730-003X

Abstract

The coronavirus disease 2019 (COVID-19) pandemic, caused by severe acute respiratory syndrome coronavirus (SARS-CoV-2) may be over, but its variants continue to emerge, and patients with mild symptoms having long COVID is still under investigation. SARS-CoV-2 infection leading to elevated cytokine levels and suppressed immune responses set off cytokine storm, fatal systemic inflammation, tissue damage, and multi-organ failure. Thus, drug molecules against virus-specific proteins that play a role in viral inflammation and simultaneous act on the host pathways participating in viral inflammation, will provide an effective antiviral therapy against emerging variants of concern. Evolutionarily conserved papain-like protease (PLpro) and main protease (Mpro) play an indispensable role in the virus life cycle and immune evasion. Direct-acting antivirals targeting both these viral proteases represent an attractive antiviral strategy that is also expected to reduce viral inflammation. The present study has evaluated the antiviral and anti-inflammatory potential of natural triterpenoids: azadirachtin, withanolide_A, and isoginkgetin. These molecules inhibit the Mpro and PLpro proteolytic activities with half-maximal inhibitory concentrations (IC_{50}) values ranging from 1.42 to 32.7 µM. Isothermal titration calorimetry (ITC) analysis validated the binding of these compounds to Mpro and PLpro. As expected, the two compounds, withanolide_A and azadirachtin exhibit potent antiviral activity with half-maximum effective concentration (EC_{50}) values of 21.73 µM and 31.19 µM, respectively. The anti-inflammatory role of azadirachtin and withanolide_A when assessed using HEK293T cells were found to significantly reduce the levels of CXCL10, TNFα, IL6, and IL8 cytokines, which are elevated in severe cases of COVID-19. Interestingly, azadirachtin and withanolide_A were also found to rescue the decreased type-I interferon response (IFN-α1). The results of this study clearly highlight the role of triterpenoids as effective antiviral molecules that target SARS-CoV-2 specific enzymes and also host immune pathways involved in virus mediated inflammation.

Keywords: SARS-CoV-2, Mpro, PLpro, cytokine storm, triterpenoids, antivirals

1. INTRODUCTION

Despite the promising vaccination programs against coronavirus disease (COVID-19), vaccine hesitancy and compromised vaccine effectiveness has contributed to breakthrough infections, waning immunity, and the recurrence of new variants of severe acute respiratory syndrome coronavirus 2 (SARS-CoV-2). With the appearance of new immune escape variants, identifying effective antivirals and druggable proteins is more critical than ever to control the inevitable outbreaks of SARS-CoV-2. Whilst there have been tremendous strides forward in identifying drugs against SARS-CoV-2, no effective treatment for COVID-19 exists to date. Identification of antivirals capable of inhibiting virus replication and interfering with host immune pathways involved in viral inflammation represents a promising avenue towards effective therapy for SARS-CoV-2 or COVID-19 patients.

Immunity dysfunction and SARS-CoV-2 infection are the two main progressions driving the pathogenesis of COVID-19 (1–3). One of the hallmark clinical feature of critically ill COVID-19 patients is the poor protective immune response with abnormally elevated levels of pro-inflammatory cytokines and chemokines such as interleukin-1 (IL-1), IL-2, IL-6, IL-8, IL-10, IL-12, IFN-γ, CXCL10, CXCL9, tumor necrosis factor-α (TNFα), etc. (3–6). Moreover, the induction of type I interferon (IFN-I; IFN-α1, IFN-β, IFN-δ, -ε, -κ, -τ) and type III interferon (IFN-III; IFN-λ1, -λ2, -λ3, and -λ4) responses are markedly impaired in severe COVID-19 patients (7–10). These dysregulated inflammatory responses lead to life-threatening pneumonia, multiorgan failure, acute respiratory distress syndrome (ARDS), and eventually death in more severe cases (2, 3, 6, 11). Since the host immune response also plays a crucial role in disease progression, anti-inflammatory therapeutics capable of upregulating host antiviral response or inhibiting the systemic inflammation may prove to be a valuable option for clinical management of the disease (12). Therefore, a combination therapy targeting both viral and host factors can be a new treatment method for mitigating COVID-19.

SARS-CoV-2 has a remarkably large (~30 kb), single-stranded RNA genome that encodes various structural, non-structural (nsP), and accessory proteins (13–15). Upon entry into the host cell, the genomic RNA is translated into pp1a and pp1ab polypeptides, which are processed by two virus-encoded cysteine proteases: the 3C-like protease (3CLpro or Mpro) and the papain-like protease (PLpro) (13–15). Subsequently, the processing of polyproteins releases 16 nsPs which compose the viral replication and transcription complex (RTC) that comprises RNA processing and proofreading function essential for maintaining the integrity of the genome (13, 15, 16). Due to the indispensable role of evolutionarily conserved Mpro and PLpro in the intracellular amplification stage of SARS-CoV-2 and other pathogenic coronaviruses such as SARS-CoV and Middle East respiratory syndrome coronavirus (MERS), direct-acting antivirals against both of these proteins represent an attractive drug design strategy.

One of the best-characterized drug targets is the multifunctional Mpro that plays an essential role in processing two polypeptides pp1a and pp1ab, by operating at 11 sites, primarily at the conserved Leu-Gln↓(Ser/Ala/Gly) sequences (the cleavage site is indicated by ↓) (17–20). Active Mpro is a homodimer containing two protomers and each protomer is composed of a catalytic region comprising a noncanonical Cys-His dyad (21). In addition, Mpro targets the RIG-1 and the

mitochondrial antiviral signaling (MAVS) protein–IFN signaling pathway to evade the innate immune responses of the host cell (22). Together with Mpro, PLpro also plays a vital role in the processing of viral polyprotein and the dysregulation of innate immune responses of the host. PLpro, a domain within nsP3, recognizes the P4-P1 consensus cleavage sequence LXGG found at the interface of nsP1/nsP2, nsP2/nsP3, and nsP3/nsP4 (23–25). This LXGG recognition sequence also resembles the sequence at the C-terminus of ubiquitin and ISG15 (23–25). Importantly, the deubiquitination and deISGylation of cellular proteins by PLpro are vital for antagonizing the antiviral pathways of the host (26, 27). The crystal structure of PLpro of SARS-CoV-2 signifies a right-handed architecture consisting of a ubiquitin-like (Ubl) domain and a "thumb-palm-finger" catalytic domain with a triad of Cys-His-Asp (24, 28). The active site of SARS-CoV-2 PLpro is conformationally and functionally conserved among other coronaviral PLpro with a flexible loop named as "blocking loop 2" that regulates the access of substrates to this site. Inhibiting the enzymatic activity of Mpro and PLpro would block the viral replication marking them as promising targets for antiviral development.

The unavailability of effective therapeutics has already exacerbated the severity of the COVID-19 pandemic. Plants have always been a rich repertoire of bioactive compounds with tremendous medicinal applications for centuries (29, 30). Compared with conventional drugs, phytopharmaceuticals from natural sources are considered a trending approach to cure ailments due to their affordability, efficacy, biocompatibility, bio-availability, and minimal side effects (31). Medicinal plants such as *Azadirachta indica*, *Withania somnifera*, *Tamarindus indica*, *Ocimum sanctum*, *Curcuma longa*, etc., are known to possess antiviral, antibacterial, or anti-cancerous activities due to the presence of phytochemicals such as flavonoids, terpenoids, limonoids, lignans, polyphenolics, coumarins, saponins, alkaloids, etc. (32–36). Of the numerous herbal plants, *Azadirachta indica* is a well-documented medicinal plant with virucidal action against human immunodeficiency virus (HIV), Chikungunya, Poliovirus, herpes simplex virus type-1 (HSV), Dengue, Chickenpox, etc. (37, 38). *Withania somnifera* also known as '*Ashwagandha*', is a prime herbal plant of Ayurvedic importance. Withanolides, a category of phytochemicals from *Withania somnifera,* have been reported to possess pharmacological activities such as an immunomodulation, prophylactic, antidepressant, anti-inflammatory, antioxidant, anti-tumor, and antiviral (39, 40). Ashwaganda's immunomodulatory properties make it a potentially useful adjunct for treatment of viral infections including Human papillomavirus infection (HPV), Hepatitis C virus (HCV), HSV, and coronaviruses – including SARS-CoV and SARS-CoV-2 (41). *Ginkgo biloba* is an antioxidant-rich herb used as an anti-tumor, antibacterial, antiviral agent, and anti-inflammatory agent (42, 43). The most commonly reported bioflavonoid from *Ginkgo biloba,* isoginkgetin, exhibits antibacterial, anti-inflammatory, anti-tumor, and antiviral activities (43, 44). Considering the multifaceted role of plant-derived phytochemicals, identification of triterpenoids against virus-specific enzymes can be a promising approach to discover potent drug candidates for COVID-19 treatment.

In previous work, our group has identified three immunomodulatory triterpenoids (Azadirachtin, withanolide_A, and isoginkgetin) as potential inhibitors of virus-encoded proteases (Mpro and PLpro) of SARS-CoV-2 using structure-assisted virtual screening and molecular dynamics approach (45, 46). Several *in silico* drug repurposing studies also predicted these triterpenoids to

target Mpro and PLpro of SARS-CoV-2. However, former predictions were based solely on computational analysis and the efficacy data from clinical trials against SARS-CoV-2 is missing (47–50). The present study investigates the antiviral and anti-inflammatory potential of identified triterpenoids in terms of Mpro and PLpro inhibition and cell-culture based SARS-CoV-2 inhibition studies. The experimentally validated lead triterpenoids identified in this study present a dual-targeting virus-directed and host-directed strategy to avenge the pandemic of COVID-19. The findings in this study demonstrate the feasibility of this multi-targeting drug design strategy and pave the way for using triterpenoids to promote disease tolerance by suppressing immune-mediated pathology and impeding replication of SARS-CoV-2.

2. MATERIALS AND METHODS

2.1 Cells, viruses, and compounds

Vero cells (NCCS Pune, India) were maintained in high-glucose Dulbecco's modified Eagle's medium (DMEM; Himedia, India) complemented with 10% fetal bovine serum (FBS; Gibco, USA), 100 units of penicillin, and 100 µg streptomycin/mL (Himedia, India). DMEM augmented with 10% FBS, 100 units of penicillin, and 100 µg streptomycin/mL was used to culture HEK293T cells (NCCS Pune, India). All cells were grown at 37 °C in a humidified atmosphere with 5% CO_2. SARS-CoV-2/Human/IND/CAD1339/2020 strain (GenBank accession no: MZ203529), isolated from SARS-CoV-2 infected Indian patient, was passaged in a culture flask of confluent Vero cells maintained in DMEM with 2% FBS (51). At the peak of infection, cell supernatant was harvested, centrifuged and further filtered through 0.22 µm filters to clarify cell debris. Virus stocks were kept at −80 °C until use. The virus was titered by end-point dilution method. All virus handling and experimental studies with live SARS-CoV-2 were conducted in Biosafety Level-3 facility at Indian Veterinary Research Institute (IVRI), Izatnagar, Bareilly, in accordance with the biosafety guidelines. Azadirachtin, withanolide_A, and isoginkgetin were procured from Cayman chemicals. Azadirachtin and withanolide_A were dissolved in methanol (Himedia, India) at 10 mM concentrations as stock solutions. Isoginkgetin was dissolved in Dimethyl sulfoxide (DMSO; Himedia, India) at 10 mM concentration.

2.2 Production of recombinant SARS-CoV-2 Mpro and PLpro

The plasmid encoding SARS-CoV-2 Mpro was a kind gift from Prof. Manidipa Banerjee, Indian Institute of Technology, Delhi. The gene corresponding to Mpro was amplified using 5'-ATATACCATGGTTAGCGGTTTTCGTAAAATGGCATTT-3' as forward primer and 5'-TAATGCTCGAGCTGAAAGGTAACACCGCTACACTGAC-3' as reverse primer. After restriction digestion with *NcoI* and *XhoI*, the gene was subcloned using *NcoI* and *XhoI* restriction sites in pET28c vector with an N-terminal histidine tag. Codon-optimized gene encoding the full-length SARS-CoV-2 PLpro (1-315 amino acids) was custom synthesized (Invitrogen, Thermo Fisher Scientific) and was cloned using *XhoI* and *NdeI* restriction sites in pET28c vector containing an N-terminal 6X histidine tag, using 5'-CAGCCATATGGAAGTTCGTACCATTAAAGT TTTTAC-3' forward primer and 5'-GGTGCTCGAGCTATTTGATGGTGGTG-3' reverse primer, as described previously (52). The recombinant constructs for PLpro and Mpro were transformed

into competent *E. coli* Rosetta cells at 37 °C in Luria Broth (LB) containing 35 μg/mL chloramphenicol and 50 μg/mL of kanamycin until the optical density (O.D.) reached 0.6. The expression of Mpro and PLpro proteins were induced using 0.5 mM isopropyl-β-d-1-thiogalactopyranoside (IPTG) at 18 °C for ~14 h. After centrifugation at 6000 rpm at 4 °C for 10 min, the PLpro and Mpro pelleted cells were resuspended in lysis buffer A (50 mM Tris-HCl, pH 8.5, 500 mM NaCl, and 5mM DTT) and lysis buffer B (50 mM Tris-HCl, pH 7.8, 150 mM NaCl), respectively. Next, the cells were lysed by French press (Constant Systems Ltd, Daventry, England), centrifuged at 10,000 rpm for 1 h, the clarified supernatants were loaded onto Ni-NTA gravity flow column (BioRad) equilibrated with binding buffer for PLpro (50 mM Tris-HCl, pH 8.5, 500 mM NaCl, and 5mM DTT) and for Mpro (20 mM Tris-HCl, pH 7.8, 20 mM NaCl, and 5mM DTT). The columns were washed with binding buffer containing 5 mM imidazole and the target proteins were eluted with an elution buffer containing 100-500 mM imidazole. 12% SDS-PAGE was run to check the purity of the purified proteins. Fractions containing pure PLpro and Mpro proteins were dialyzed against buffer C (50 mM Tris pH 8.5, 150 mM NaCl and 1 mM DTT) and buffer D (20 mM HEPES, pH 7.8, 20 mM NaCl, 1 mM DTT), respectively. The proteins were concentrated using 10 kDa cut off Amicon centrifugal filters (Millipore, USA).

2.3 Enzyme activity assay and IC_{50} determination

To determine the half-maximal inhibitory concentrations (IC_{50}) of inhibitors against Mpro and PLpro, a fluorescence-based cleavage assays were developed using fluorogenic substrate peptides. Dabcyl-AVLQSGFR-Glu-Edans (Biolinkk, India) for Mpro and Z-RLRGG-7-amido-4-methylcoumarin (Biolinkk, India) based on the C-terminal residues of ubiquitin, for PLpro. The proteolytic activity assays for PLpro and Mpro were performed in reaction buffer A (20 mM Tris-HCl pH 7.5, 150 mM NaCl) and reaction buffer B (20 mM Tris-HCl pH 7.8, 20 mM NaCl) respectively. The non-binding black 96-well microtiter plates (Corning) with a final reaction volume of 100 μL were used. The activity of SARS-CoV-2 was assessed by adding 1 μM purified enzymes to the plate followed by initiation of enzymatic reaction with the addition of 1.5 μM fluorogenic substrate peptides. The released fluorescence signals were monitored using a Synergy HT plate reader (BioTek Instruments, Inc) with wavelength filters for 360/40 nm (excitation) and 460/40 nm (emission). Inhibition of enzymatic activity of SARS-CoV-2 Mpro and PLpro were assayed by preincubating purified Mpro and PLpro proteins with compounds for 30 min at 25 °C. The substrate peptides were added in the last step at a final concentration of 1 μM/well. Upon the addition of substrate, the fluorescence signals were monitored at 360 nm (excitation) and 460 nm (emission). Measured fluorescence signals were blank-corrected with buffer containing different concentrations of the compounds incubated with the substrate without purified Mpro and PLpro enzymes. Data from duplicate sets of readings were plotted as dose inhibition curves to determine the IC_{50} values of compounds. Graph pad prism (version 8.3.1) and Microsoft Excel were used to analyze and prepare graphs.

2.4 Estimation of binding affinities by ITC

The dissociation constant and thermodynamic parameters for the affinity of compounds with proteases were determined using a MicroCal ITC200 micro calorimeter (Malvern, Northampton, MA). Binding of PLpro and Mpro with the compounds were measured in buffer A (50 mM Tris

pH 8.5, 150 mM NaCl and 1 mM DTT) and buffer B (20 mM HEPES pH 8.0, 20 mM NaCl and 1 mM DTT), respectively. Titrations of Mpro were performed with 50 μM protein in the cell and 500 μM of inhibitors in the syringe at 25 °C. To test the binding between PLpro and compounds, 5 μM PLpro in the cell was titrated against 1 mM concentration of inhibitors in the syringe at 25 °C. For PLpro, a 0.5 μL priming injection followed by 13 consecutive 3 μl injections of compounds were titrated into 350 μL sample cell at 25 °C with 180 s intervals using a stirring rate of 750 rpm. For Mpro, a 0.5 μL priming injection followed by 15 consecutive 2.5 μl injections of compounds were titrated into 350 μL sample cell at 25 °C with 180 s intervals using a stirring rate of 750 rpm. All samples were gently vacuum-degassed before experiments. After subtracting the controls, the isotherm curves were fitted to a single-site binding model and the data was analysis was done using the Microcal Origin software provided by the manufacturer.

2.5 Cell viability assay

Cell viability profile of selected compounds was assayed in uninfected, compound-treated cells using MTT (3-(4, 5-dimethylthiazolyl-2)-2,5-diphenyltetrazolium bromide) assay. Monolayers of 4×10^4 Vero cells/well in a 96-well plate were cultured in DMEM augmented with 10% FBS followed by an overnight incubation at 37 °C. On the next day, the media over cells was removed and fresh medium containing serially diluted compounds was added to each well of the plate followed by an incubation at 37 °C and 5% CO_2. After 48 h of compound treatment, 20 μL of MTT reagent (5 mg/mL) (Himedia, India) was added to each well which was subsequently incubated for 4 h at 37 °C and 5% CO_2 in the dark. Post incubation, the media was discarded and the formazan salt crystals were dissolved using 150 μL/well of DMSO. As readouts, absorbance values were measured at 550 nm using a Synergy HT plate reader (BioTek Instruments, Inc). Measurements from 0.1% DMSO-treated cells were included as positive control to calculate percent cytotoxicity for each compound. All treatments were made in triplicates. The CC_{50} (50% cytotoxic concentration) was calculated from the dose-response curve in GraphPad Prism 8.

2.6 Drug treatment and viral load reduction assay

To evaluate the antiviral spectrum of azadirachtin, withanolide_A, and isoginkgetin, Vero cells were seeded into 24-well cell-culture plate and were allowed to grow to confluency for 24 h at 37 °C and 5% CO_2. Before virus inoculation, the cells were pre-treated with different doses of compounds for 3 h. Post incubation, the media containing compound was removed and the cells were washed with Phosphate Buffered Saline (PBS) (Himedia, India). SARS-CoV-2 at a multiplicity of infection (MOI) of 0.1 was added and incubated for 1.5 h. The virus inoculum was then removed and the cells were rewashed with PBS. Furthermore, fresh compound-containing DMEM with 2% FBS was added. An equivalent volume of the methanol or DMSO solvent was added to virus control. At 48 h post-infection, the plate was freeze-thawed and the viral RNA in the cell lysate was extracted using HiPurA™ Viral RNA Purification Kit, according to the manufacturer's instructions. The gene expression for Viral RNA in the cell lysate was quantified using quantitative real-time PCR (qRT-PCR) with the SARS-CoV-2-specific primers using the commercially available COVISure-COVID-19 Real-Time PCR kit (Genetix) according to the manufacturer’s protocol. Data was acquired using the following conditions: 15 min at 50 °C, a denaturation step at 95 °C for 2 min, 40 cycles of denaturation at 95 °C for of 30 s, and finally annealing at 60 °C for 30 s. All treatments were performed in duplicates for each compound.

Percentage inhibition versus concentration graphs were plotted after normalizing the data using GraphPad Prism software to determine IC_{50} values.

2.7 Virus quantification assay

The production of infectious virus in compound treated cells and SARS-CoV-2 infected cells in comparison to only infected cells was quantified by tissue culture infectious dose 50 ($TCID_{50}$) assay as reported previously (52). Vero cells were plated at a density of 4×10^4 cells/well in a 96-well plate and the plate was incubated overnight at 37 °C in a 5% CO_2 incubator to reach 80-90% confluency. The cellular monolayer was then exposed to 10-fold serial dilutions (10^1 to 10^8) of freeze-thawed lysate of cells infected and treated with compounds, collected at 48 h post-infection of the antiviral assay. Cells were incubated for 3 to 4 days at 37 °C in an incubator with 5% CO_2. Cells were regularly observed for the appearance of obvious cytopathic effects (CPE). Mock-treated and infected samples were used as positive control, and samples with only cell-culture media were used as a negative control. After incubation, the viral inoculum was removed and the cells were fixed by the addition of 10% formaldehyde for 2 h followed by staining with 0.5% crystal violet solution. Virus endpoint titer was determined using the Reed-Muench method and expressed as log $TCID_{50}$/mL.

2.8 Pro-inflammatory cytokine quantification assay

To ascertain the anti-inflammatory roles of selected triterpenoids, cell-based assays using HEK293T cells were optimized. In brief, HEK293T cells were seeded in 24-well plate at a density of 5.0×10^4 cells per well in 10% DMEM supplemented 100 units of penicillin, and 100 µg streptomycin/mL and were incubated for 24 h for adherence. At a confluency of ~80%, the cells were pre-treated with azadirachtin (75 µM) and withanolide_A (50 µM) diluted in OptiMEM media (Gibco). After an incubation period of 2 h, the compound containing media was removed and the cells were stimulated with 1 µg/mL of Polyinosinic:polycytidylic acid (poly I:C; Sigma) using Lipofectamine 2000 (Invitrogen) for 6 h. Post incubation, the media over the cells was removed, fresh OptiMEM (Gibco) containing the compounds was added to cells, and the plate was incubated at 37 °C for 24 h. Untreated cells were included as controls. Total RNA was isolated from the cells using TRIzol (RNAiso; Takara) by following manufacturer's instructions. In total, 1 µg RNA was subsequently converted to cDNA using random hexamer primer using PrimeScript™ 1st strand cDNA Synthesis Kit (Takara Bio) in accordance with manufacturer's protocol. Gene expression analyses for IL6, IL-8, CXCL10, TNFα, and IFN-α1 cytokines were performed using KAPA SYBR fast universal qPCR kit (Sigma-Aldrich, USA) on QuantStudio real-time PCR system (Applied Biosystems, IN) following manufacturer's instructions. Based on the ΔΔCt method, the relative expression of targeted genes was represented as fold changes with β-actin as endogenous control for normalization. All reactions were carried duplicates in a 96-well plate (Applied Biosystems, IN). Fold change was calculated by taking mock-treated cells as 1.

The primer sequences used for qRT-PCR are as follows:

Gene	Forward primer	Reverse primer

IFN-α1	5′-GGAGTTTGATGGCAACCAGT-3′	5′-CTCTCCTCCTGCATCACACA-3′
IL6	5′-GCAGAAAAAGGCAAAGAATC-3′	5′-CTACATTTGCCGAAGAGC-3′
IL8	5′-ATGACTTCCAAGCTGGCCGTGGCT-3′	5′- TCTCAGCCCTCTTCAAAAACTTCTC-3′
CXCL10	5′-TGGCATTCAAGGAGTACCTC-3′	5′-TTGTAGCAATGATCTCAACACG-3′
TNFα	5′- AGCCTCTTCTCCTTCCTGATCGTG-3′	5′- GGCTGATTAGAGAGAGGTCCCTGG-3′
β-actin	5′-ATTGCCGACAGGATGCAGAA-3′	5′-GCTGATCCACATCTGCTGGAA-3'

3. RESULTS

3.1 The potency of triterpenoids as a dual inhibitor against Mpro and PLpro

To dissect the inhibitory potential of the selected triterpenoids against SARS-CoV-2 proteases, a fluorescence resonance energy transfer (FRET)-based assays were optimized for Mpro and PLpro. To accomplish this, gene sequences corresponding to Mpro and PLpro were cloned into the pET28c vector and were expressed in the *E. coli* expression system. Mpro and PLpro proteins were purified with Ni-NTA column to high purity. To establish the FRET assay condition and to determine the inhibitory potency of identified compounds, fluorogenic substrate peptides corresponding to the cleavage sites for Mpro and PLpro were used. The inhibitory potency of azadirachtin, withanolide_A, and isoginkgetin was tested against the proteolytic activity of Mpro and PLpro of SARS-CoV-2 using the developed FRET assays. The selected triterpenoids displayed potent inhibitory activities against both the viral enzymes: the Mpro and PLpro, when tested in a concentration range of 0.1 to 100 µM. Dose-response experiments determined the IC_{50} values of azadirachtin, withanolide_A, and isoginkgetin by varying the compound concentrations against Mpro and PLpro of SARS-CoV-2. Withanolide_A, azadirachtin, and isoginkgetin inhibited the proteolytic activity of SARS-CoV-2 Mpro with IC_{50} values of 32.70 ± 3.20 µM, 19.85 ± 6.12 µM, and 21.34 ± 4.46 µM, respectively (Figure 1). For PLpro of SARS-CoV-2, the IC_{50} values 1.42 ± 0.57 µM, 15.56 ± 0.51 µM, and 7.5 ± 0.56 µM, were observed for withanolide_A, azadirachtin, and isoginkgetin respectively (Figure 1).

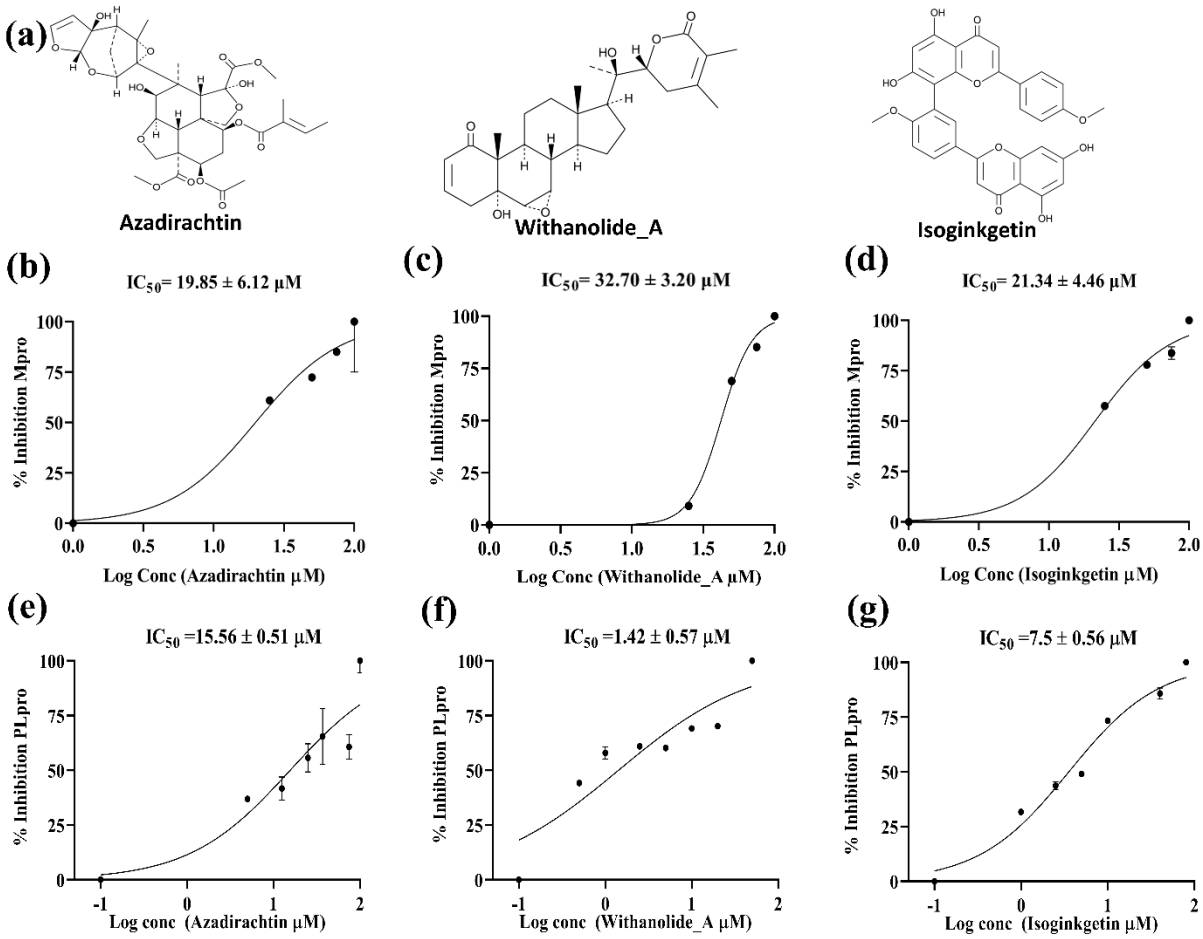

FIGURE 1: (a) Chemical structures of triterpenoids. (b, c, d) The inhibitory potencies of azadirachtin, withanolide_A, and isoginkgetin against the enzymatic activity of Mpro. (e, f, g) The inhibitory potencies of azadirachtin, withanolide_A, and isoginkgetin against the enzymatic activity of PLpro. Dose–response curves for IC_{50} values were determined by nonlinear regression fit. The calculated enzymatic activity with each compound was normalized to control. All data are shown as mean ± standard error, n = 2 biological replicates.

3.2 Estimation of binding affinities by ITC

To validate the binding of selected triterpenoids with SARS-CoV-2 PLpro and Mpro, the binding affinities with respective proteases were assessed using ITC. The thermodynamic data fitted into a one-site binding model revealed binding affinity (K_D), of SARS-CoV-2 Mpro with withanolide_A, azadirachtin, and isoginkgetin as 127 µM, 88.4 µM, and 144 µM, respectively (Table 1 and figure 2). With regard to SARS-CoV-2 PLpro, the ITC experiments revealed K_D values of 478 µM, 641 µM, and 169 µM for withanolide_A, azadirachtin, and isoginkgetin respectively. The results of thermodynamic parameters are documented in Table 1. Moreover, the 1:1 stoichiometry (N) detected postulates specificity for a single binding site of Mpro and PLpro (Table 1). The binding of withanolide_A, azadirachtin, and isoginkgetin to SARS-CoV-2 PLpro and Mpro is exothermically driven as shown by their enthalpy variation (ΔH) (Table 1 and figure 2). As depicted in Figure 2 and Table 1, the measured thermodynamic parameters and the titration curves revealed good binding affinities of Mpro and PLpro with the selected triterpenoids, which nicely corroborates with the data from FRET assay.

Table 1: Thermodynamic binding parameters of azadirachtin, withanolide_A, and isoginkgetin for purified PLpro and Mpro of SARS-CoV-2.

Compound	No. of sites (N)	K_D (µM)	ΔH (cal/mol)	ΔS (cal/ mol/ degree)
PLpro				
Withanolide_A	1	478	$-2.952\times10^{7} \pm 5.136\times 10^{6}$	-9.90×10^{4}
Azadirachtin	1	641	$-2.927 \times10^{5}\pm 1.1$	-9.67×10^{2}
Isoginkgetin	1	169	$-4.949 \times 10^{6} \pm 1.55$	-1.66×10^{4}
Mpro				
Withanolide_A	1	127	$-2.47\times10^{6} \pm 9.031\times10^{4}$	-8.27×10^{3}
Azadirachtin	1	88.4	$-1.631\times10^{5} \pm 1.89\times10^{4}$	-5.29×10^{2}
Isoginkgetin	1	144	$-1.641\times10^{6} \pm 2.809\times10^{5}$	-5.49×10^{3}

N: binding stoichiometry; K_D*: equilibrium dissociation constant; ΔH: enthalpy variation; ΔS: entropy variation; SD: standard-deviation;*

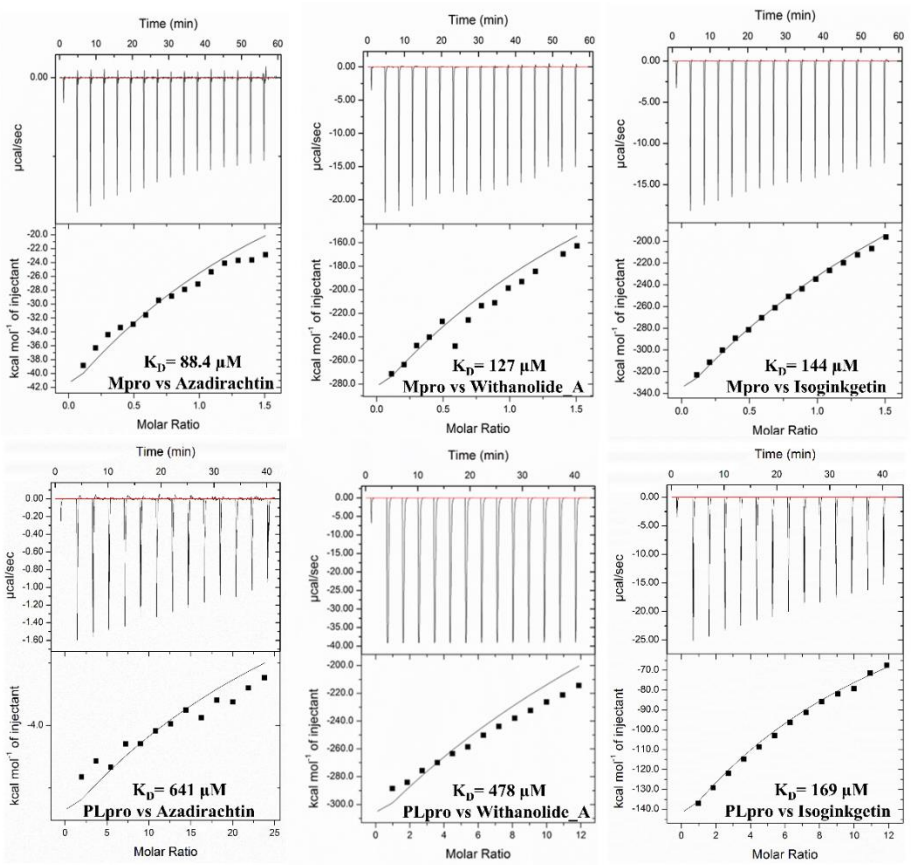

FIGURE 2: Binding analysis of azadirachtin, withanolide_A, and isoginkgetin with SARS-CoV-2 Mpro and PLpro characterized by ITC. The top of each ITC titration is its raw data and the bottom represents the binding isotherm fitted to one sets of site model. K_D values are inset.

3.3 Triterpenoids inhibit SARS-CoV-2 *in vitro*

To further authenticate the enzyme inhibition and ITC results, the capability of the selected compounds to inhibit SARS-CoV-2 *in vitro* was evaluated. Among the tested inhibitors, withanolide_A and azadirachtin displayed no cytotoxicity at tested concentrations (Figure 3). The CC_{50} values of both withanolide_A and azadirachtin are above 100 µM, indicating a good safety window for these triterpenoids. However, there was an observed increase in cellular cytotoxicity in the presence of the compound isoginkgetin at concentrations of more than 1 µM (Supplementary figure S1). To determine the effectiveness of triterpenoids on SARS-CoV-2, Vero cells were treated with withanolide_A, azadirachtin, and isoginkgetin and viral infection was quantified by qRT-PCR using primers specific for the RNA-dependent RNA polymerase (RdRp) and Nucleocapsid protein. Percent inhibition data were normalized to the infected controls (solvent DMSO or methanol treated as well as infected cells) and cell-only control (Solvent DMSO or methanol treated). The percent cytotoxicity data was normalized to cell only control (solvent DMSO or methanol treated). In line with previous observations, cell-based assays revealed that treatment with withanolide_A and azadirachtin resulted in significant inhibitory potential against SARS-CoV-2 with a half-maximum effective concentration (EC_{50}) value of 21.73 µM and 31.19 µM, respectively. Furthermore, both compounds harbored discernable dose-dependent antiviral activities with a percentage inhibition of more than 90% (Figure 3). However, the compound isoginkgetin was not observed to inhibit the replication of SARS-CoV-2 at its non-toxic concentrations (Supplementary figure S1). Consistent with these viability assay results, the high cytotoxicity for isoginkgetin observed in this study is in accordance with other published studies (43).

Encouraged by the promising antiviral activity of withanolide_A and azadirachtin, a further set of experiments were performed to determine the $TCID_{50}$ for azadirachtin and withanolide_A. Treatment with azadirachtin reduced virus titer from 5.5 log $TCID_{50}$/mL to 2 log $TCID_{50}$/mL (Figure 3). Withanolide_A decreased the viral titer to 4 log $TCID_{50}$/mL compared to mock-treated virus control (5.5 log $TCID_{50}$/mL) (Figure 3). Indeed, a more significant decrease in infectious viral progenies was observed when virus-infected cells were treated with higher concentrations of azadirachtin fold (3.5 log reduction $TCID_{50}$/mL) in comparison to withanolide_A (decrease of 1.5 log $TCID_{50}$/mL) (Figure 3). The results obtained from the $TCID_{50}$ assay demonstrated a dose-dependent decrease in infectious viral titer. Collectively, the data provides strong evidence that azadirachtin and withanolide_A could potentially impede SARS-CoV-2 replication *in vitro*.

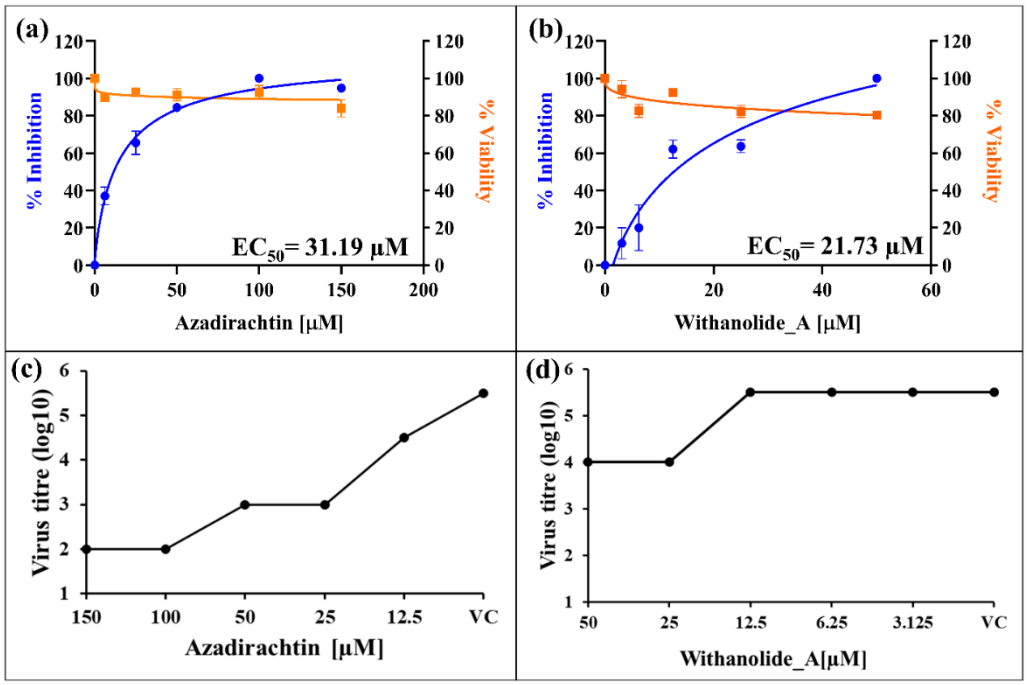

FIGURE 3: Immunomodulatory triterpenoids reduce SARS-CoV-2 infection. Vero cells were infected with SARS-CoV-2 (0.1 MOI) in the presence of indicated concentrations of compounds for 48 h followed by the quantification of viral RNA copies by qRT-PCR and $TCID_{50}$ assay. Cytotoxicity of compounds on Vero cells was measured using the MTT assay. (a and b) Percent inhibition of SARS-CoV-2 by azadirachtin and withanolide_A on Vero cells (represented in blue) and percent viability of azadirchtin and withanolide_A in Vero cells (represented in orange). Values are represented as mean ± SD of two independent experiments. Error bars corresponds to the standard deviation from duplicate experiments. (c and d) SARS-CoV-2 viral titer after treatment with triterpenoids. Confluent monolayer of Vero cells in a 96-well plate were inoculated with 10-fold serial dilutions of samples harvested from virus yield reduction assay and the plate was incubated for 3-4 days until the appearance of cytopathic effect (CPE). After its incubation period, 10% formaldehyde was used to fix the cells and staining was done using crystal violet solution. Data is expressed as log $TCID_{50}$/mL.

3.4 Anti-inflammatory role of Azadirachtin and withanolide_A

SARS-CoV-2 infections are often associated with highly elevated levels of pro-inflammatory cytokines, including IL-6, IL-1, IL-8, IL-10, IL-12, TNFα, IFN-γ, CXCL10, and CXCL9 that in many cases lead to severe lung damage and multiorgan failure (2–5, 11, 53). Previous studies have also reported lymphopenia, neutrophilia, reduced or delayed type I interferon responses (IFNα and IFNβ) and hyperproduction of pro-inflammatory cytokines, which are primarily responsible for aggravating immunopathological complications in COVID-19 patients (7–10). Therefore, an immunomodulatory therapy to control the virus-triggered exuberant cytokine release can provide wide-spectrum effect in controlling SARS-CoV-2 infection and resuming host's homeostasis. For this reason, the inhibitory effects of azadirachtin and withanolide_A on the expression of inflammatory mediators stimulated by treatment with poly I:C, a synthetic analog of dsRNA that mimics virus infection was investigated. Cellular lysates collected after 24 h of poly I:C stimulation were quantified for the levels of cytokine production (CXCL10, TNFα, IL6, IL8, and IFN-α1) using qRT-PCR. The stimulation of HEK293T cells with Poly I:C dramatically increased the levels of pro-inflammatory cytokines CXCL10, TNFα, IL6, and IL8 when compared with

untreated cellular control (Figure 4). Interestingly, the mRNA expression levels of CXCL10, TNFα, IL6, and IL8 upregulated in response to poly I:C were observably decreased after treatment with azadirachtin and withanolide_A (Figure 4). Further analysis also showed that treatment with azadirachtin and withanolide_A also restored the levels of IFN-α1, that are reported to be remarkably reduced in COVID-19 patients (Figure 4) (3, 7). Altogether, the data from SARS-CoV-2 antiviral assays and anti-inflammatory studies speculate that these triterpenoids inhibit both viral replication as well as the expression of inflammatory genes.

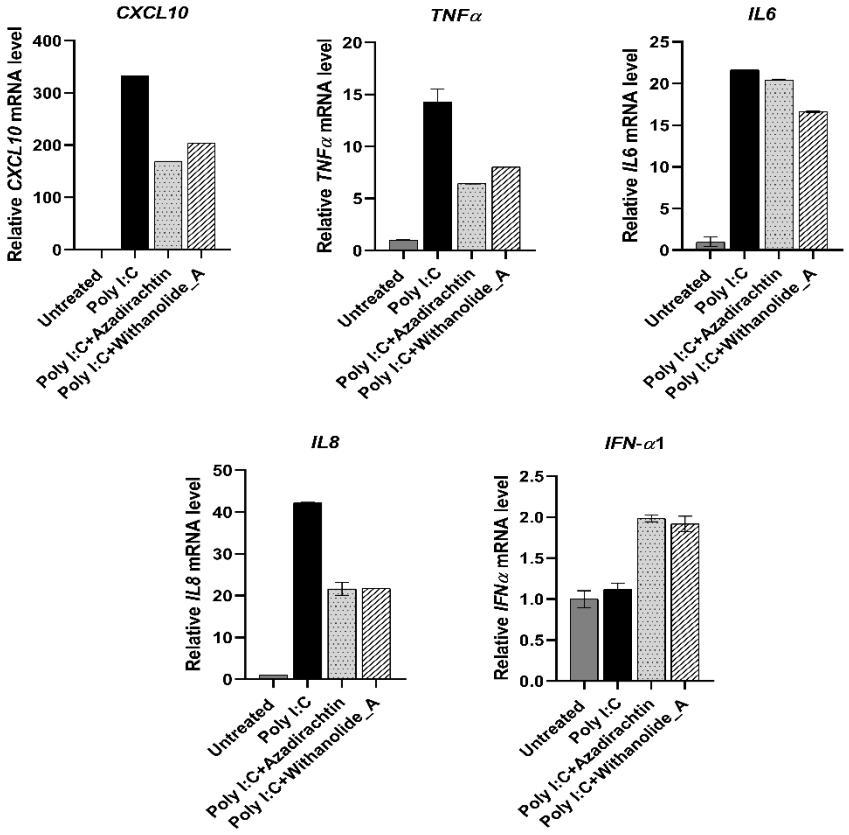

FIGURE 4: Anti-inflammatory effects of azadirachtin and withanolide_A. HEK293T cells pre-treated with azadirachtin (75 µM) and withanolide_A (50 µM) for 2h, followed by stimulation with Poly I:C (1 µg/mL) for 6 h. Post incubation, the cells were allowed to grow in fresh medium containing compounds. 24 h post poly I:C treatment, the total RNA was extracted and the relative fold change of CXCL10, TNFα, IL6, IL8, and IFN-α1 was determined using qRT-PCR. Expression of each gene was normalized to endogenous control β-actin and gene expression for untreated cells was taken as a reference. Shown are the data for mean ± SD of duplicate reactions.

4. DISCUSSION

In the setting of waning immunity from antibody-based interventions for SARS-CoV-2, broadly effective antiviral therapies with multiple modes of action have increased in importance and might become an important tool in fight against the COVID-19 pandemic. Despite advances in modern vaccine and therapeutics, the landscape of effective treatment options against SARS-CoV-2 is still underdeveloped. So far, the U.S. Food and Drug Administration (FDA) approved treatment options against SARS-CoV-2 includes remdesivir, molnupiravir, and paxlovid, which are reported to shorten COVID-19 hospitalization times, but exhibited limited efficacy in clinical use (54–57). The requirement for effective antiviral therapies is still a crucial aspect for timely management of viral infection and to improve the preparedness for future outbreaks of SARS-CoV-2 or its other emerging variants (58, 59). A strategy combining virus-specific and host-targeted antivirals can potentially offer effective antiviral therapies to combat emerging variants of SARS-CoV-2 and to reduce the virus induced inflammatory responses in mild to severely infected COVID-19 patients (60, 61). SARS-CoV-2 specific proteases, the Mpro and PLpro, are of particular interest for developing effective antiviral therapies because of their fundamental roles in viral replication and evasion of innate immune responses (18, 19, 23, 62–64). Additionally, the conservation of substrate-binding pockets in both proteases across coronaviruses is expected to provide effective therapeutic interventions to treat COVID-19 amid the emergence of new variants (64).

Of importance, medicinal plants offer a rich reserve of phytochemicals with immense therapeutic potentiality as antimicrobial, antiviral, anti-tumor, anti-inflammatory, neuroprotective, cardioprotective, and immunomodulatory effects (29, 30, 32, 33, 65). The triterpenoids are an important class of secondary metabolites from natural sources with wide-spectrum pharmacological activities including antiviral, antibacterial, anti-tumor, anti-cancer, anti-microbials, etc. (30, 42, 43, 49, 66–70) Triterpenoids have also been found to play immunomodulatory or anti-inflammatory roles highlighting their potential in management of immunological complications (32, 39, 40, 44, 49, 71). In this study, the three triterpenoids (azadirachtin, withanolide_A, and isoginkgetin) which were earlier identified by *in-silico* analysis targeting the SARS-CoV-2 virus specific proteases (Mpro and PLpro), have been further investigated for their antiviral as well as anti-inflammatory roles (45, 46). Given that the triterpenoids target the active site of both proteases (45, 46), the direct inhibitory effects on enzymatic activities of Mpro and PLpro were measured using an *in vitro* fluorescence-based protease assay. The selected compounds displayed multi-potent inhibitory effects against proteolytic activities of both Mpro and PLpro of SARS-CoV-2 with IC_{50} values in the low micromolar range (Figure 1).

To investigate the binding affinities and stoichiometry of inhibitors to Mpro and PLpro, ITC experiments were conducted that confirmed the stoichiometry of the compounds for a single binding site (Figure 2). The data from the ITC experiment revealed good binding affinities of Mpro with the K_D as 88.4 μM, 127 μM, and 144 μM, for azadirachtin, withanolide_A, and Isoginkgetin, respectively (Figure 2, Table 1), which nicely corroborates with the result of Mpro proteolytic assay. The binding affinities of PLpro with withanolide_A, azadirachtin, and isoginkgetin was also examined that revealed K_D values of 478 μM, 641 μM, and 169 μM, respectively (Figure 2

and Table 1). Treatment with azadirachtin and withanolide_A exhibited robust antiviral effects in *in vitro* cell-based assays against SARS-CoV-2 with EC_{50} values of 31.19 µM and 21.73 µM, respectively (Figure 3). Hemdan *et al*. proposed the antiviral activity of extracts from leaves and bark of *Azadirachta indica* against SARS-CoV-2, however the exact mechanism of action was not provided (66). The present study identified azadirachtin, an important triterpenoid from *Azadirachta indica*, to be one of the bioactive molecules responsible for exhibiting inhibitory activity against SARS-CoV-2 and its proteases. Consistent with previously published reports, the compound isoginkgetin displayed considerably higher cytotoxicity (43), and was not observed to inhibit viral replication in Vero cells in this study at concentrations lower than those exhibiting cytotoxicity (Supplementary figure S1).

Infection with SARS-CoV-2 can lead to an overexuberant immune response that can lead to severe pneumonia, cytokine storm, multiorgan dysfunction, and eventually death (2–4, 11). A dysregulated immune response associated with attenuated IFN responses and overproduction of inflammatory cytokines or chemokines (CXCL10, TNFα, IL6, IL8) has been proposed to be a prime reason for cytokine storm or ARDS (1–3, 7). Therapies focused on modulating innate immune responses to attenuate the excessive release of pro-inflammatory cytokines or to promote the IFN antiviral response represent a noteworthy target for treating patients with severe COVID-19 (72, 73). Published literature suggests a wide-spectrum of pharmacological properties of both Azadirachtin and withanolide_A such as anticancer, anti-inflammatory, antiviral, antibacterial, and immunomodulators (32, 33, 39, 40, 68, 69). Owing to the significant inhibitory effects against SARS-CoV-2 and safer toxicity profiles, only azadirachtin and withanolide_A were selected for further studies. To ascertain the roles of withanolide_A and azadirachtin on virus-triggered inflammatory pathways, HEK293T cells were treated with poly I:C, a TLR3 agonist, that mimics virus infection and induces inflammatory responses in the host cells (67, 74, 75). Findings in this study revealed that treatment with azadirachtin and withanolide_A decreased the levels of CXCL10, TNFα, IL6, IL8 that are well documented to be modulated in critically ill COVID-19 patients (Figure 4). Previous studies have shown the regulatory roles of SARS-CoV-2 Mpro and PLpro in delayed type I IFN responses as an immune evasion strategy (22, 27, 64, 76). Interestingly, both compounds were able to rescue the decreased IFN-α1 responses, which could possibly be due to inhibition of both Mpro or PLpro or any other off-target in signaling cascade (Figure 4). Altogether, the present study supports the notion that triterpenoids effectively inhibit the enzymatic activity of Mpro and PLpro, reduce SARS-CoV-2 viral load, and reduces inflammatory signatures.

Considering the dual inhibitory effect of withanolide_A and azadirachtin on both viral replication and inflammatory markers, the findings from this study evidently suggests that the triterpenoids could efficiently inhibit the replication of SARS-CoV-2 and ameliorate cytokine storm induced immunological injuries. The favorable profiles and SARS-CoV-2 antiviral activity of withanolide_A and azadirachtin supports further *in vivo* and clinical testing for the treatment of COVID-19.

AUTHOR CONTRIBUTIONS

ST, PK, PKP, and GKS planned and designed the study together. ST, PK, and GKS supervised the experimental work. ST, PK, PKP, and GKS analyzed and discussed the results. SC, AS, and SN performed the experiments, analyzed the data with critical inputs from ST, PK, GKS, and PKP. The manuscript was prepared by ST, PK, GKS, SC, AS, PKP, and SN. All authors read and approved the final manuscript.

ACKNOWLEDGMENTS

This work was supported by funding from Science and Engineering Research Board, Department of Science & Technology, Government of India (Project reference no. IPA/2020/000054). We thank Prof. Manidipa Banerjee for providing Mpro plasmid. SC thank Council of Scientific & Industrial Research, Government of India for financial support. AS and SN acknowledges the Ministry of Human Resource Development, (MHRD) for financial support. The authors acknowledge and thank the Macromolecular Crystallographic Facility (MCU) at IIC, Indian Institute of Technology, Roorkee.

CONFLICT OF INTEREST

The authors have no conflicts of interest to declare.

REFERENCES

[1] Hafezi, B., Chan, L., Knapp, J. P., Karimi, N., Alizadeh, K., et al. (2021) Cytokine Storm Syndrome in SARS-CoV-2 Infections: A Functional Role of Mast Cells. Cells 10, 1761–1765.

[2] Hu, B., Huang, S., and Yin, L. (2021) The cytokine storm and COVID-19. Journal of Medical Virology 93, 250–256.

[3] Yang, L., Xie, X., Tu, Z., Fu, J., Xu, D., et al. (2021) The signal pathways and treatment of cytokine storm in COVID-19. Signal Transduction and Targeted Therapy 6, 255.

[4] Costela-Ruiz, V. J., Illescas-Montes, R., Puerta-Puerta, J. M., Ruiz, C., and Melguizo-Rodríguez, L. (2020) SARS-CoV-2 infection: The role of cytokines in COVID-19 disease. Cytokine & Growth Factor Reviews 54, 62–75.

[5] Neufeldt, C. J., Cerikan, B., Cortese, M., Frankish, J., Lee, J.-Y., et al. (2022) SARS-CoV-2 infection induces a pro-inflammatory cytokine response through cGAS-STING and NF-κB. Communications Biology 5, 45.

[6] Li, S., Zhang, Y., Guan, Z., Li, H., Ye, M., et al. (2020) SARS-CoV-2 triggers inflammatory responses and cell death through caspase-8 activation. Signal Transduction and Targeted Therapy 5, 235.

[7] Hadjadj, J., Yatim, N., Barnabei, L., Corneau, A., Boussier, J., et al. (2020) Impaired type I interferon activity and inflammatory responses in severe COVID-19 patients. Science 369, 718–724.

[8] Bastard, P., Zhang, Q., Zhang, S.-Y., Jouanguy, E., and Casanova, J.-L. (2022) Type I interferons and SARS-CoV-2: from cells to organisms. Current Opinion in Immunology 74, 172–182.

[9] Kindler, E., and Thiel, V. (2016) SARS-CoV and IFN: Too Little, Too Late. Cell Host & Microbe 19, 139–141.

[10] Kim, Y.-M., and Shin, E.-C. (2021) Type I and III interferon responses in SARS-CoV-2 infection. Experimental & Molecular Medicine 53, 750–760.

[11] Sun, X., Wang, T., Cai, D., Hu, Z., Chen, J., et al. (2020) Cytokine storm intervention in the early stages of COVID-19 pneumonia. Cytokine & Growth Factor Reviews 53, 38–42.

[12] Zhou, Y.-W., Xie, Y., Tang, L.-S., Pu, D., Zhu, Y.-J., et al. (2021) Therapeutic targets and interventional strategies in COVID-19: mechanisms and clinical studies. Signal Transduction and Targeted Therapy 6, 317.

[13] V'kovski, P., Kratzel, A., Steiner, S., Stalder, H., and Thiel, V. (2021) Coronavirus biology and replication: implications for SARS-CoV-2. Nature Reviews Microbiology 19, 155–170.

[14] Gordon, D. E., Jang, G. M., Bouhaddou, M., Xu, J., Obernier, K., et al. (2020) A SARS-CoV-2 protein interaction map reveals targets for drug repurposing. Nature 583, 459–468.

[15] Dubey, A., Choudhary, S., Kumar, P., and Tomar, S. (2021) Emerging SARS-CoV-2 Variants: Genetic Variability and Clinical Implications. Current Microbiology 79, 20.

[16] Rani, R., Long, S., Pareek, A., Dhaka, P., Singh, A., et al. (2022) Multi-target direct-acting SARS-CoV-2 antivirals against the nucleotide-binding pockets of virus-specific proteins. Virology 577, 1–15.

[17] Anand, K., Ziebuhr, J., Wadhwani, P., Mesters, J. R., and Hilgenfeld, R. (2003) Coronavirus Main Proteinase (3CLpro) Structure: Basis for Design of Anti-SARS Drugs. Science 300, 1763–1767.

[18] Zhang, L., Lin, D., Sun, X., Curth, U., Drosten, C., et al. (2020) Crystal structure of SARS-CoV-2 main protease provides a basis for design of improved α-ketoamide inhibitors. Science 368, 409–412.

[19] Günther, S., Reinke, P. Y. A., Fernández-García, Y., Lieske, J., Lane, T. J., et al. (2021) X-ray screening identifies active site and allosteric inhibitors of SARS-CoV-2 main protease. Science 372, 642–646.

[20] Rani, R., Singh, A., Pareek, A., and Tomar, S. (2020) In silico guided drug repurposing to combat SARS-CoV-2 by Targeting Mpro, the key virus specific protease.

[21] Wenhao, D., Bing, Z., Xia-Ming, J., Haixia, S., Jian, L., et al. (2020) Structure-based design of antiviral drug candidates targeting the SARS-CoV-2 main protease. Science 368, 1331–1335.

[22] Yongzhen, L., Chao, Q., Youliang, R., Chau, N., J, F. J., et al. (2021) SARS-CoV-2 Nsp5 Demonstrates Two Distinct Mechanisms Targeting RIG-I and MAVS To Evade the Innate Immune Response. mBio 12, e02335-21.

[23] Klemm, T., Ebert, G., Calleja, D. J., Allison, C. C., Richardson, L. W., et al. (2020) Mechanism and inhibition of the papain-like protease, PLpro, of SARS-CoV-2. The EMBO Journal 39, e106275.

[24] Fu, Z., Huang, B., Tang, J., Liu, S., Liu, M., et al. (2021) The complex structure of GRL0617 and SARS-CoV-2 PLpro reveals a hot spot for antiviral drug discovery. Nature Communications 12, 488.

[25] McClain, C. B., and Vabret, N. (2020) SARS-CoV-2: the many pros of targeting PLpro. Signal Transduction and Targeted Therapy 5, 223.

[26] Zong, Z., Zhang, Z., Wu, L., Zhang, L., and Zhou, F. (2021) The Functional Deubiquitinating Enzymes in Control of Innate Antiviral Immunity. Advanced Science 8, 2002484.

[27] Shin, D., Mukherjee, R., Grewe, D., Bojkova, D., Baek, K., et al. (2020) Papain-like protease regulates SARS-CoV-2 viral spread and innate immunity. Nature 587, 657–662.

[28] Osipiuk, J., Azizi, S.-A., Dvorkin, S., Endres, M., Jedrzejczak, R., et al. (2021) Structure of papain-like protease from SARS-CoV-2 and its complexes with non-covalent inhibitors. Nature Communications 12, 743.

[29] Balunas, M. J., and Kinghorn, A. D. (2005) Drug discovery from medicinal plants. Life Sciences 78, 431–441.

[30] Perumal Samy, R., and Gopalakrishnakone, P. (2010) Therapeutic Potential of Plants as Anti-Microbials for Drug Discovery. Evidence-Based Complementary and Alternative Medicine 7, 260483.

[31] Parasuraman Subramani (2018) Herbal Drug Discovery: Challenges and Perspectives. Current Pharmacogenomics and Personalized Medicine 16, 63–68.

[32] Zeenat Fahmeeda, R. M. S. A. W. and A. I. (2018) Therapeutic, phytochemistry and pharmacology of Azadirachta indica: A review. International Journal of Unani and Integrative Medicine 2, 20–28.

[33] Rayees, S., and Malik, F. (2017) Withania somnifera: From Traditional Use to Evidence Based Medicinal Prominence. In Science of Ashwagandha: Preventive and Therapeutic Potentials. pp. 81–103, Springer International Publishing.

[34] Kaur, R., Neetu, Mudgal, R., Jose, J., Kumar, P., et al. (2019) Glycan-dependent chikungunya viral infection divulged by antiviral activity of NAG specific chi-like lectin. Virology 526, 91–98.

[35] Choudhary, S., Neetu, N., Singh, V. A., Kumar, P., Chaudhary, M., et al. (2021) Chikungunya virus titration, detection and diagnosis using N-Acetylglucosamine (GlcNAc) specific lectin based virus capture assay. Virus Research 302, 198493.

[36] Cohen MM (2014) Tulsi - Ocimum sanctum: A herb for all reasons. Journal of Ayurveda and Integrative medicine 5, 251–259.

[37] Tiwari, V., Darmani, N. A., Yue, B. Y. J. T., and Shukla, D. (2010) In vitro antiviral activity of neem (Azardirachta indica L.) bark extract against herpes simplex virus type-1 infection. Phytotherapy Research 24, 1132–1140.

[38] Parida, M. M., Upadhyay, C., Pandya, G., and Jana, A. M. (2002) Inhibitory potential of neem (Azadirachta indica Juss) leaves on Dengue virus type-2 replication. Journal of Ethnopharmacology 79, 273–278.

[39] Verma, S. K., and Kumar, A. (2011) Therapeutic uses of withania somnifera (Ashwagandha) with a note on withanolides and its pharmacological actions.

[40] Paul, S., Chakraborty, S., Anand, U., Dey, S., Nandy, S., et al. (2021) Withania somnifera (L.) Dunal (Ashwagandha): A comprehensive review on ethnopharmacology, pharmacotherapeutics, biomedicinal and toxicological aspects. Biomedicine & Pharmacotherapy 143, 112175.

[41] Kashyap, V. K., Dhasmana, A., Yallapu, M. M., Chauhan, S. C., and Jaggi, M. (2020) Withania somnifera as a potential future drug molecule for COVID-19. Future Drug Discovery 2, FDD50.

[42] Haruyama, T., and Nagata, K. (2013) Anti-influenza virus activity of Ginkgo biloba leaf extracts. Journal of Natural Medicines 67, 636–642.

[43] Jessica, T., Mena, A.-N., Armin, F., T, S. M., Stephanie, P., et al. (2019) Isoginkgetin, a Natural Biflavonoid Proteasome Inhibitor, Sensitizes Cancer Cells to Apoptosis via Disruption of Lysosomal Homeostasis and Impaired Protein Clearance. Molecular and Cellular Biology 39, e00489-18.

[44] Darrigrand, R., Pierson, A., Rouillon, M., Renko, D., Boulpicante, M., et al. (2021) Isoginkgetin derivative IP2 enhances the adaptive immune response against tumor antigens. Communications Biology 4, 269.

[45] Sharma, M., Mahto, J. K., Dhaka, P., Neetu, N., Tomar, S., et al. (2022) MD simulation and MM/PBSA identifies phytochemicals as bifunctional inhibitors of SARS-CoV-2. Journal of Biomolecular Structure and Dynamics 40, 12048–12061.

[46] Kumar, K. A., Sharma, M., Dalal, V., Singh, V., Tomar, S., et al. (2021) Multifunctional inhibitors of SARS-CoV-2 by MM/PBSA, essential dynamics, and molecular dynamic investigations. Journal of Molecular Graphics and Modelling 107, 107969.

[47] Dhanjal, J. K., Kumar, V., Garg, S., Subramani, C., Agarwal, S., et al. (2021) Molecular mechanism of anti-SARS-CoV2 activity of Ashwagandha-derived withanolides. International Journal of Biological Macromolecules 184, 297–312.

[48] Patil, V. S., Hupparage, V. B., Malgi, A. P., Deshpande, S. H., Patil, S. A., et al. (2021) Dual inhibition of COVID-19 spike glycoprotein and main protease 3CLpro by Withanone from Withania somnifera. Chinese Herbal Medicines 13, 359–369.

[49] Khanal, P., Chikhale, R., Dey, Y. N., Pasha, I., Chand, S., et al. (2022) Withanolides from Withania somnifera as an immunity booster and their therapeutic options against COVID-19. Journal of Biomolecular Structure and Dynamics 40, 5295–5308.

[50] Chakraborty, S., Mallick, D., Goswami, M., Guengerich, F. P., Chakrabarty, A., et al. (2022) The Natural Products Withaferin A and Withanone from the Medicinal Herb Withania somnifera Are Covalent Inhibitors of the SARS-CoV-2 Main Protease. Journal of Natural Products 85, 2340–2350.

[51] Dhaka, P., Singh, A., Choudhary, S., Kumar, P., Sharma, G. K., et al. (2022) Discovery of anti-SARS-CoV-2 molecules using structure-assisted repurposing approach targeting N-protein. bioRxiv, 2022.03.12.484092.

[52] Choudhary, S., Nehul, S., Kumar, K. A., Sharma, S., Rani, R., et al. (2022) Crystal structure and activity profiling of deubiquitinating inhibitors-bound to SARS-CoV-2 papain like protease revealed new allosteric sites for antiviral therapies. bioRxiv, 2022.11.11.516107.

[53] Catanzaro, M., Fagiani, F., Racchi, M., Corsini, E., Govoni, S., et al. (2020) Immune response in COVID-19: addressing a pharmacological challenge by targeting pathways triggered by SARS-CoV-2. Signal Transduction and Targeted Therapy 5, 84.

[54] Beigel, J. H., Tomashek, K. M., Dodd, L. E., Mehta, A. K., Zingman, B. S., et al. (2020) Remdesivir for the Treatment of Covid-19 — Final Report. New England Journal of Medicine 383, 1813–1826.

[55] Wang, M., Cao, R., Zhang, L., Yang, X., Liu, J., et al. (2020) Remdesivir and chloroquine effectively inhibit the recently emerged novel coronavirus (2019-nCoV) in vitro. Cell Research 30, 269–271.

[56] Wang, Y., Zhang, D., Du, G., Du, R., Zhao, J., et al. (2020) Remdesivir in adults with severe COVID-19: a randomised, double-blind, placebo-controlled, multicentre trial. The Lancet 395, 1569–1578.

[57] Kabinger, F., Stiller, C., Schmitzová, J., Dienemann, C., Kokic, G., et al. (2021) Mechanism of molnupiravir-induced SARS-CoV-2 mutagenesis. Nature Structural & Molecular Biology 28, 740–746.

[58] Singh, M., and de Wit, E. (2022) Antiviral agents for the treatment of COVID-19: Progress and challenges. Cell Reports Medicine 3, 100549.

[59] Burki, T. K. (2022) The role of antiviral treatment in the COVID-19 pandemic. The Lancet Respiratory Medicine 10, e18.

[60] Chitalia, V. C., and Munawar, A. H. (2020) A painful lesson from the COVID-19 pandemic: the need for broad-spectrum, host-directed antivirals. Journal of Translational Medicine 18, 390.

[61] Maarifi, G., Martin, M.-F., Zebboudj, A., Boulay, A., Nouaux, P., et al. (2022) Identifying enhancers of innate immune signaling as broad-spectrum antivirals active against emerging viruses. Cell Chemical Biology 29, 1113-1125.e6.

[62] Kiira, R., Scott, P., Jun, T., Katrina, S., Melissa, C., et al. (2008) A noncovalent class of papain-like protease/deubiquitinase inhibitors blocks SARS virus replication. Proceedings of the National Academy of Sciences 105, 16119–16124.

[63] Wioletta, R., Zongyang, L., Mikolaj, Z., Stephanie, P., Digant, N., et al. (2021) Activity profiling and crystal structures of inhibitor-bound SARS-CoV-2 papain-like protease: A framework for anti–COVID-19 drug design. Science Advances 6, eabd4596.

[64] Wu, Y., Ma, L., Zhuang, Z., Cai, S., Zhao, Z., et al. (2020) Main protease of SARS-CoV-2 serves as a bifunctional molecule in restricting type I interferon antiviral signaling. Signal Transduction and Targeted Therapy 5, 221.

[65] Sharma, V., Kaushik, S., Pandit, P., Dhull, D., Yadav, J. P., et al. (2019) Green synthesis of silver nanoparticles from medicinal plants and evaluation of their antiviral potential against chikungunya virus. Applied Microbiology and Biotechnology 103, 881–891.

[66] Hemdan, B. A., Mostafa, A., Elbatanony, M. M., El-Feky, A. M., Paunova-Krasteva, T., et al. (2023) Bioactive Azadirachta indica and Melia azedarach leaves extracts with anti-SARS-CoV-2 and antibacterial activities. PLOS ONE 18, e0282729-.

[67] Zhang, X., Chen, L., Hu, C., Fast, D., Zhang, L., et al. (2022) Curcumin attenuates poly(I:C)-induced immune and inflammatory responses in mouse macrophages by inhibiting TLR3/TBK1/IFNB cascade. Journal of Functional Foods 89, 104949.

[68] Sarkar, L., Oko, L., Gupta, S., Bubak, A. N., Das, B., et al. (2022) Azadirachta indica A. Juss bark extract and its Nimbin isomers restrict β-coronaviral infection and replication. Virology 569, 13–28.

[69] Gupta, M., and Kaur, G. (2016) Aqueous extract from the Withania somnifera leaves as a potential anti-neuroinflammatory agent: a mechanistic study. Journal of Neuroinflammation 13, 193.

[70] Nayak, D., Ashe, S., Rauta, P. R., Kumari, M., and Nayak, B. (2016) Bark extract mediated green synthesis of silver nanoparticles: Evaluation of antimicrobial activity and antiproliferative response against osteosarcoma. Materials Science and Engineering C 58, 44–52.

[71] Behl, T., Kumar, K., Brisc, C., Rus, M., Nistor-Cseppento, D. C., et al. (2021) Exploring the multifocal role of phytochemicals as immunomodulators. Biomedicine & Pharmacotherapy 133, 110959.

[72] Puhl, A. C., Gomes, G. F., Damasceno, S., Fritch, E. J., Levi, J. A., et al. (2022) Vandetanib Blocks the Cytokine Storm in SARS-CoV-2-Infected Mice. ACS Omega 7, 31935–31944.

[73] Dobosh, B., Zandi, K., Giraldo, D. M., Goh, S. L., Musall, K., et al. (2022) Baricitinib attenuates the proinflammatory phase of COVID-19 driven by lung-infiltrating monocytes. Cell Reports 39, 110945.

[74] Gao, X., Chan, P. K. S., Lui, G. C. Y., Hui, D. S. C., Chu, I. M.-T., et al. (2021) Interleukin-38 ameliorates poly(I:C) induced lung inflammation: therapeutic implications in respiratory viral infections. Cell Death & Disease 12, 53.

[75] Mukherjee, R., Bhattacharya, A., Bojkova, D., Mehdipour, A. R., Shin, D., et al. (2021) Famotidine inhibits toll-like receptor 3-mediated inflammatory signaling in SARS-CoV-2 infection. Journal of Biological Chemistry 297.

[76] Chen, X., Yang, X., Zheng, Y., Yang, Y., Xing, Y., et al. (2014) SARS coronavirus papain-like protease inhibits the type I interferon signaling pathway through interaction with the STING-TRAF3-TBK1 complex. Protein & Cell 5, 369–381.

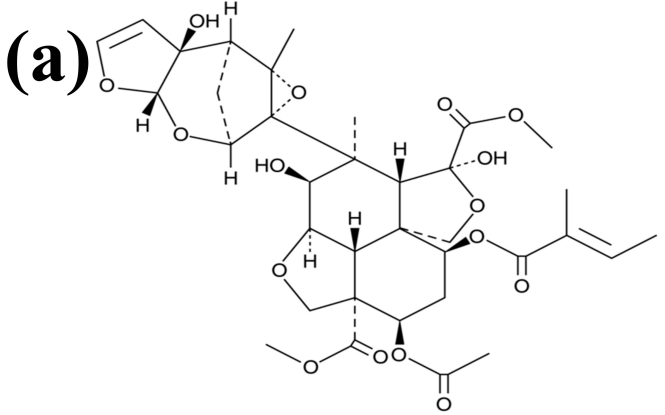
(a)
Azadirachtin

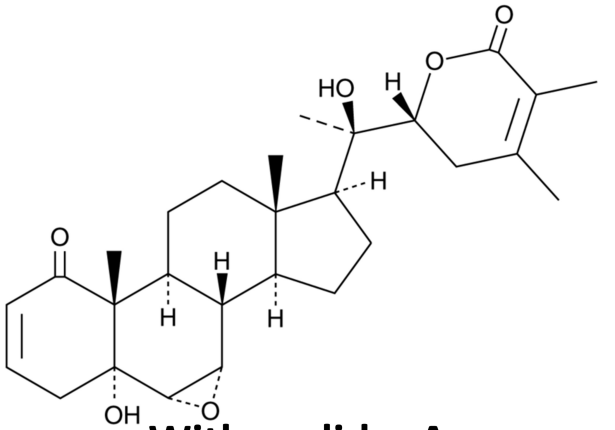
Withanolide_A

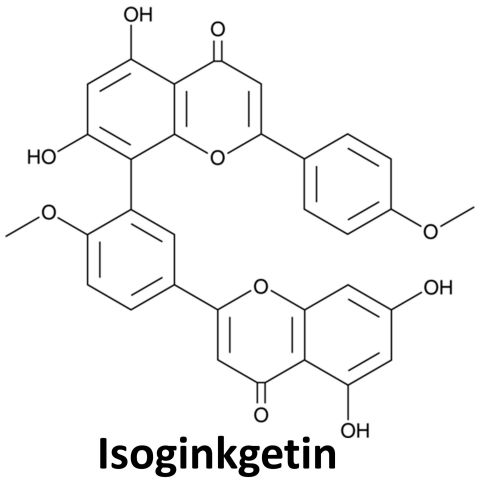
Isoginkgetin

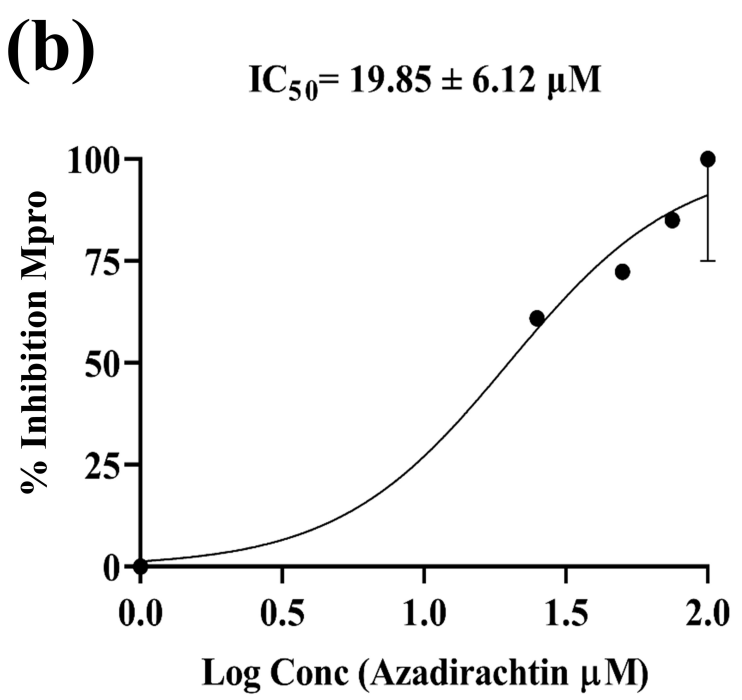
(b)
IC50= 19.85 ± 6.12 μM
% Inhibition Mpro
Log Conc (Azadirachtin μM)

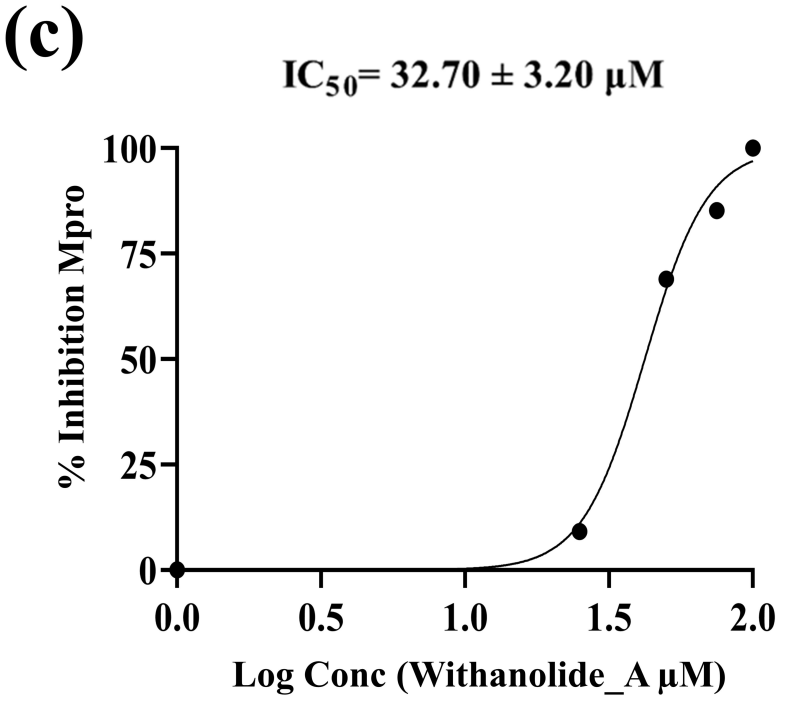
(c)
IC50= 32.70 ± 3.20 μM
% Inhibition Mpro
Log Conc (Withanolide_A μM)

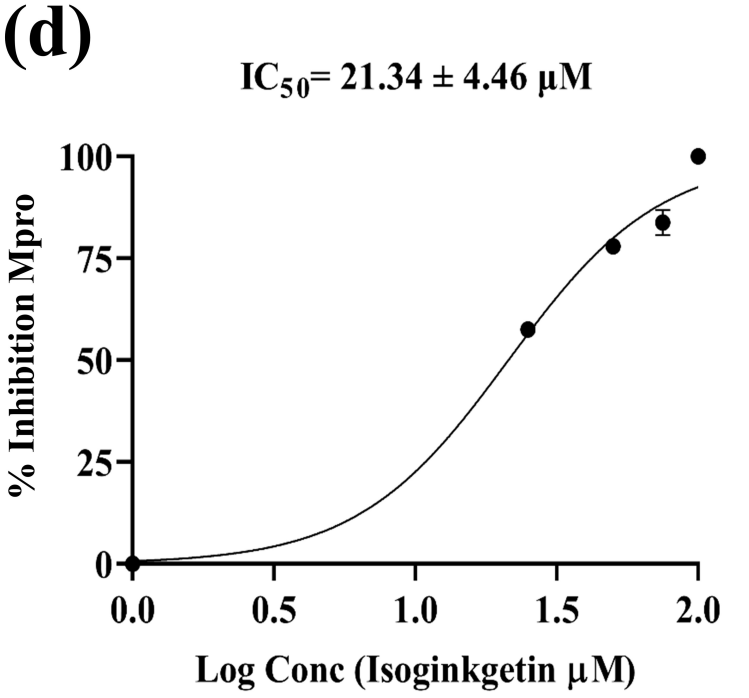
(d)
IC50= 21.34 ± 4.46 μM
% Inhibition Mpro
Log Conc (Isoginkgetin μM)

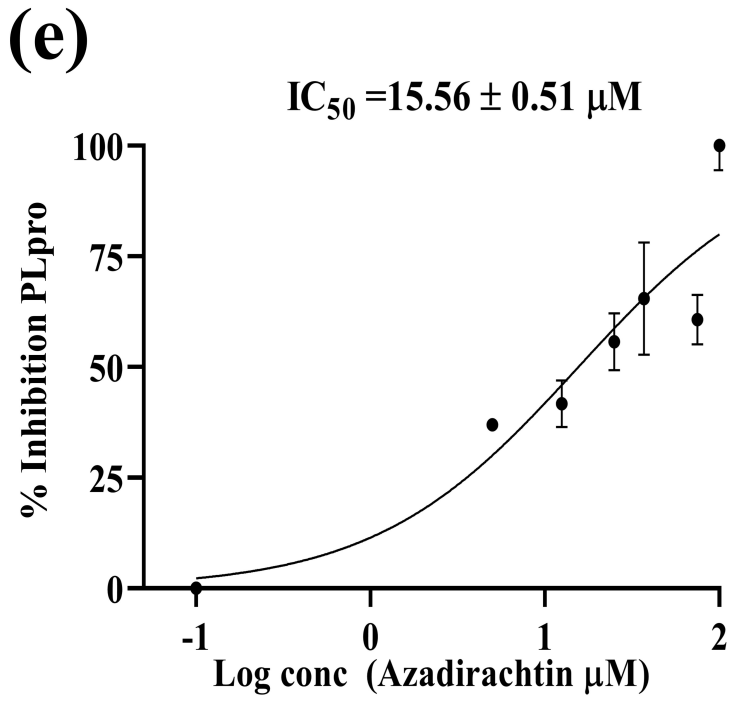
(e)
IC50 =15.56 ± 0.51 μM
% Inhibition PLpro
Log conc (Azadirachtin μM)

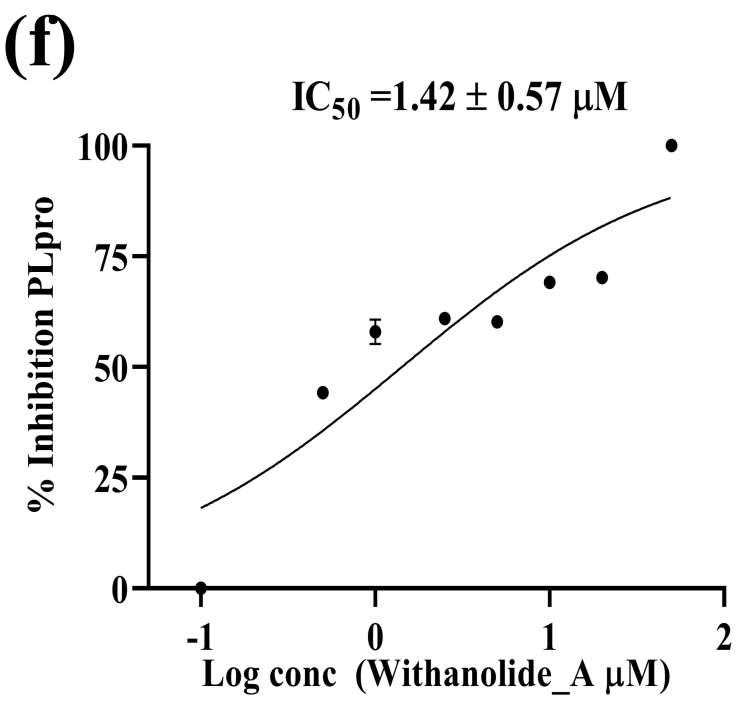
(f)
IC50 =1.42 ± 0.57 μM
% Inhibition PLpro
Log conc (Withanolide_A μM)

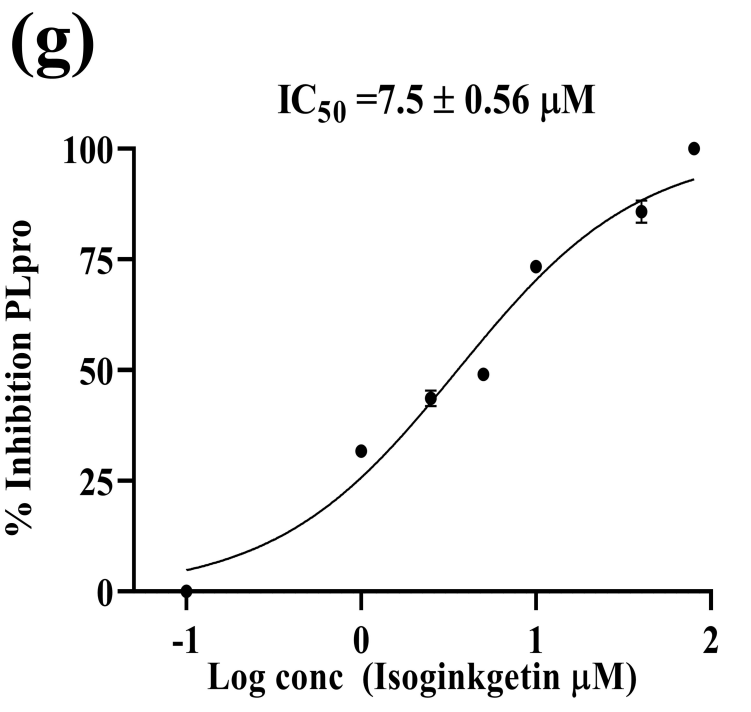
(g)
IC50 =7.5 ± 0.56 μM
% Inhibition PLpro
Log conc (Isoginkgetin μM)

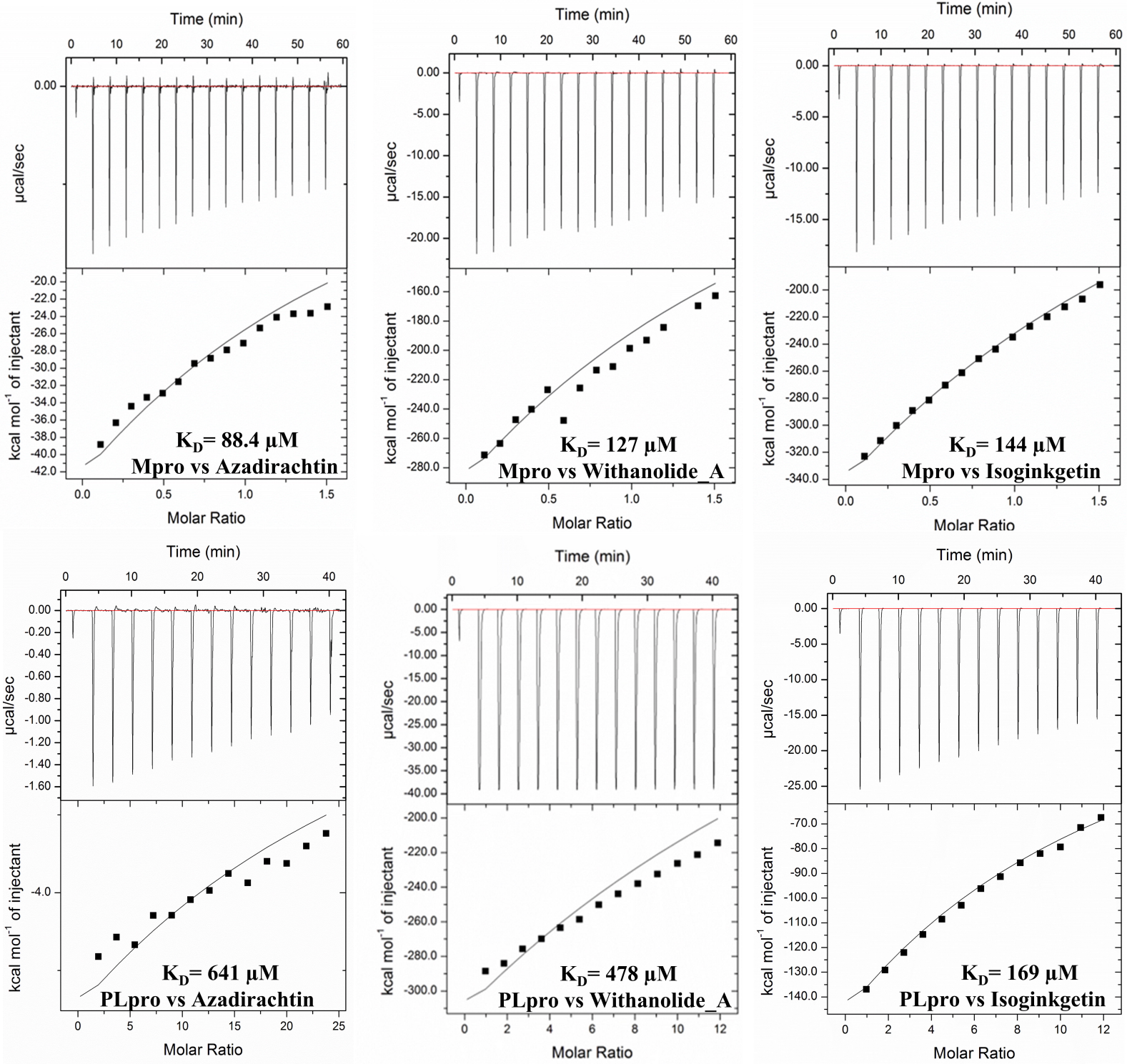
Time (min)
µcal/sec
kcal mol^{-1} of injectant
Molar Ratio
K_D= 88.4 µM
Mpro vs Azadirachtin
K_D= 127 µM
Mpro vs Withanolide_A
K_D= 144 µM
Mpro vs Isoginkgetin
K_D= 641 µM
PLpro vs Azadirachtin
K_D= 478 µM
PLpro vs Withanolide_A
K_D= 169 µM
PLpro vs Isoginkgetin

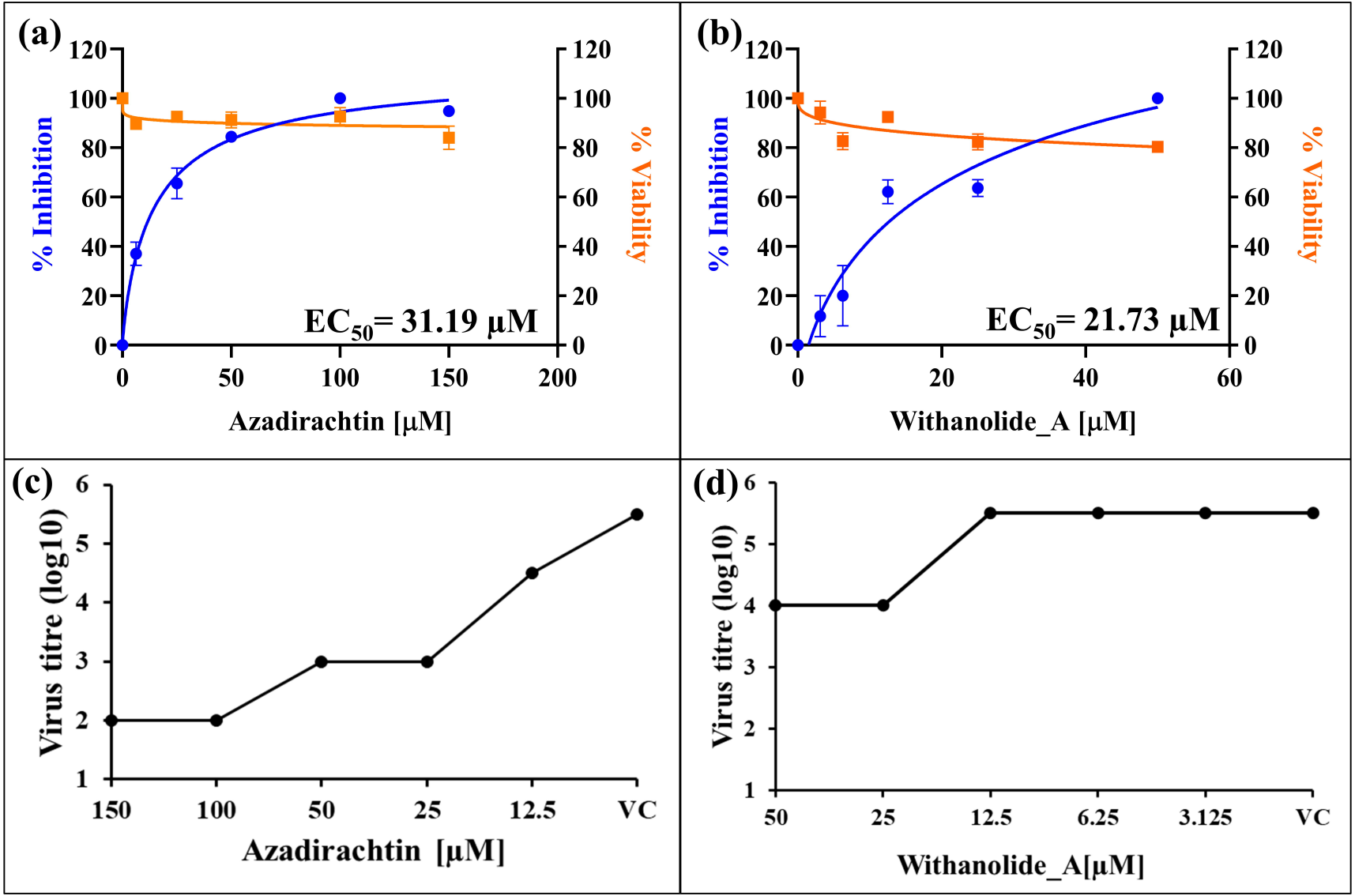
(a)
% Inhibition
% Viability
EC50= 31.19 µM
Azadirachtin [µM]
(b)
% Inhibition
% Viability
EC50= 21.73 µM
Withanolide_A [µM]
(c)
Virus titre (log10)
Azadirachtin [µM]
150
100
50
25
12.5
VC
(d)
Virus titre (log10)
Withanolide_A[µM]
50
25
12.5
6.25
3.125
VC

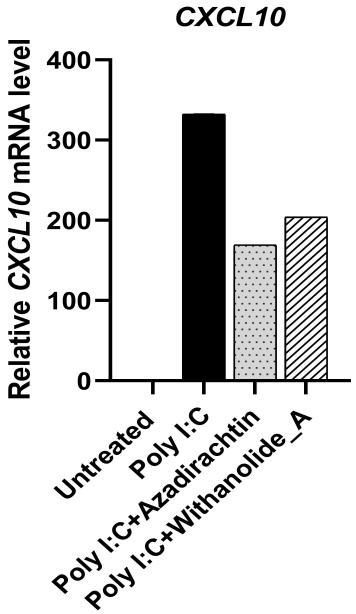
CXCL10
Relative CXCL10 mRNA level
400
300
200
100
0
Untreated
Poly I:C
Poly I:C+Azadirachtin
Poly I:C+Withanolide_A

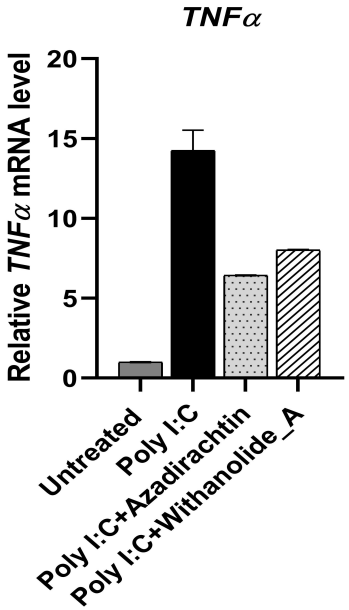
TNFα
Relative TNFα mRNA level
20
15
10
5
0
Untreated
Poly I:C
Poly I:C+Azadirachtin
Poly I:C+Withanolide_A

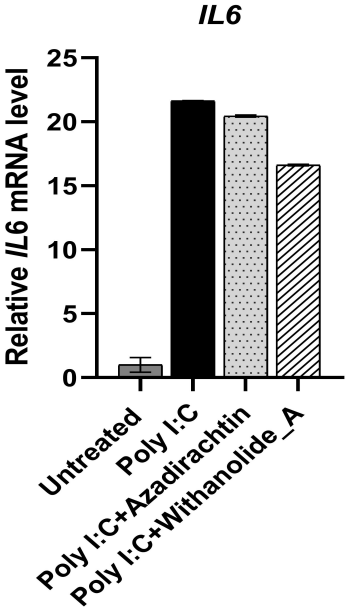
IL6
Relative IL6 mRNA level
25
20
15
10
5
0
Untreated
Poly I:C
Poly I:C+Azadirachtin
Poly I:C+Withanolide_A

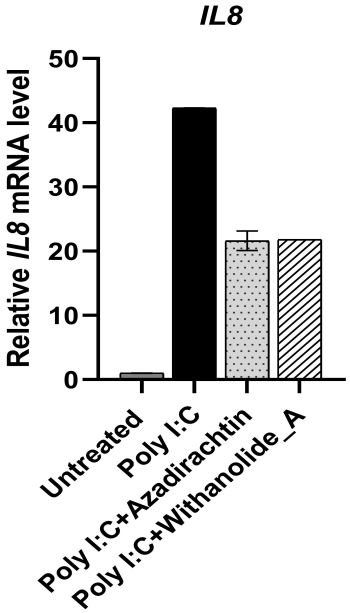
IL8
Relative IL8 mRNA level
50
40
30
20
10
0
Untreated
Poly I:C
Poly I:C+Azadirachtin
Poly I:C+Withanolide_A

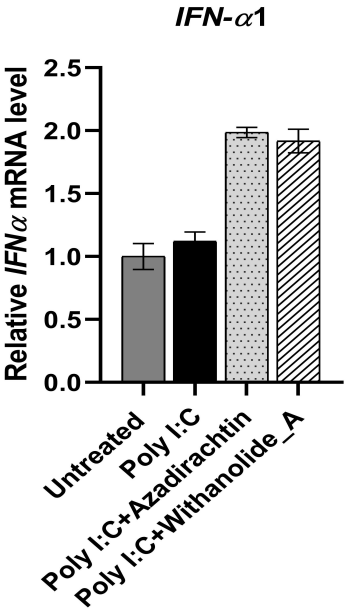
IFN-α1
Relative IFNα mRNA level
2.5
2.0
1.5
1.0
0.5
0.0
Untreated
Poly I:C
Poly I:C+Azadirachtin
Poly I:C+Withanolide_A